Nonisothermal Melt-Crystallization Kinetics of Syndiotactic Polypropylene Compounded with Various Nucleating Agents

Paninlada Charoenphol, Pitt Supaphol

Conductive and Electroactive Polymers Research Unit and The Petroleum and Petrochemical College, Chulalongkorn University, Soi Chula 12, Phyathai Road, Pathumwan, Bangkok 10330, Thailand

Received 6 April 2004; accepted 1 August 2004
DOI 10.1002/app.21259
Published online in Wiley InterScience (www.interscience.wiley.com).

ABSTRACT: Nonisothermal melt-crystallization behavior of syndiotactic polypropylene (sPP) compounded with 5% by weight (wt %) of some inorganic fillers [i.e., kaolin, talcum, marl, titanium dioxide (TiO_2), and silicon dioxide (SiO_2)] and 1 wt % of some organic fillers, which are some sorbital derivatives (i.e., DBS, MDBS, and DMDBS) was investigated and reported for the first time. It was found that the ability of these fillers to nucleate sPP decreased in the following sequence: DBS > talcum > MDBS > SiO_2 ~ kaolin ~ DMDBS > marl > TiO_2, with DBS being able to shift the crystallization exotherm by ~ 18°C on average, while TiO_2 was able to shift the crystallization exotherm by only ~ 6°C on average, from that of neat sPP. The Avrami analysis revealed that the Avrami exponent for sPP compounds varied between 2.9 and 4.3, with the values for neat sPP varying between 3.1 and 6.8. Lastly, the Ziabicki's crystallizability of sPP compounds was greater than that of neat sPP, suggesting an increase in the crystallization ability of sPP as a result of the presence of these fillers. © 2004 Wiley Periodicals, Inc. J Appl Polym Sci 95: 245–253, 2005

Key words: syndiotactic; polypropylene; crystallization; nucleation

INTRODUCTION

Syndiotactic polypropylene (sPP) of high regio- and stereoregularities was successfully synthesized using the metallocene catalyst system by Ewen et al.,[1] instead of the traditional Ziegler–Natta catalyst system.[2] This led to renewed interest in this polymer.[3–8] Despite some of its interesting properties, such as high ductility and high optical transparency, the syndiotactic form of PP (i.e., sPP) has enjoyed less commercial success than its isotactic counterpart (iPP).[9]

Among a number of drawbacks, the slow crystallization rate of sPP is an important factor limiting commercial utilization of this polymer.[10] Studies related to the crystallization process of semicrystalline polymers are of great importance in polymer processing, because the resulting physical properties of the products are strongly related to the extent of crystallization and the morphology formed. Both quiescent isothermal and nonisothermal melt-crystallization studies revealed that sPP is a slowly crystallizing polymer.[10–12] Addition of nucleating agents may help to enhance the crystallization rates by providing more sites for nucleation, hence reducing the cycle time. Nucleating agents are either inorganic or organic in their chemical makeup. Some examples for inorganic nucleating agents are talcum, mica, barium sulfate ($BaSO_4$), and calcium carbonate ($CaCO_3$); whereas, some examples for organic agents are sorbitals and their derivatives.

In the present contribution, a differential scanning calorimeter (DSC) was used to study nonisothermal melt-crystallization of neat sPP and sPP compounded with an inorganic filler [i.e., kaolin, talcum, marl, titanium dioxide (TiO_2), or silicon dioxide (SiO_2)] and an organic one that is a sorbitol derivative (i.e., DBS, MDBS, or DMDBS). The experimental data are analyzed based on the Avrami and Ziabicki macrokinetic models.

THEORETICAL BACKGROUND

The overall isothermal crystallization kinetics is often analyzed by the Avrami model,[13–15] in which the relative crystallinity as a function of time $\theta(t)$ can be expressed in the following form:

$$\theta(t) = 1 - \exp\lfloor -(K_a t)^n \rfloor \in [0,1], \quad (1)$$

where K_a and n_a are the Avrami crystallization rate constant and the Avrami exponent, respectively. Usually, the Avrami rate constant K_a is written in the form of the composite Avrami rate constant k_a (i.e., $k_a = K_a^n$); however, use of K_a is more preferable since its units are given as an inverse of time. Both K_a and n_a are constants specific to a given crystalline morphol-

Correspondence to: P. Supaphol (pitt.s@chula.ac.th).

Journal of Applied Polymer Science, Vol. 95, 245–253 (2005)

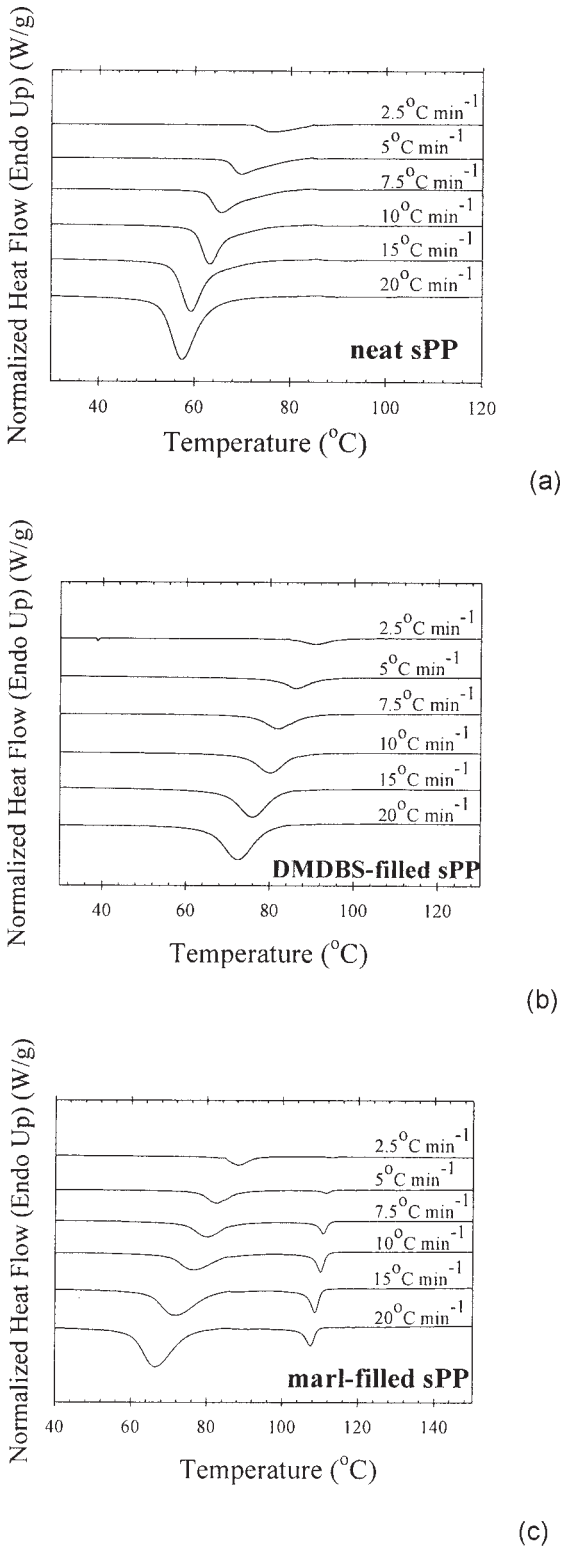

Figure 1 Nonisothermal melt-crystallization exotherms of (a) neat sPP and sPP compounded with (b) 1 wt % DMDBS and (c) 5 wt % marl for six different cooling rates ranging from 2.5 to 20°C/min.

ogy and type of nucleation for a particular crystallization condition.[16]

In the study of nonisothermal crystallization using DSC, the energy released during the crystallization process appears to be a function of temperature rather than time. As a result, the relative crystallinity as a function of temperature $\theta(T)$ can be formulated as

$$\theta(T) = \frac{\int_{T_o}^{T} \left(\frac{dH_c}{dT}\right) dT}{\Delta H_c}, \qquad (2)$$

where T_o and T represent the onset and an arbitrary temperature, respectively, dH_c is the enthalpy of crystallization released during an infinitesimal temperature range dT, and ΔH_c is the overall enthalpy of crystallization for a specific cooling condition.

To use eq. (1) in the analysis of nonisothermal crystallization data obtained by DSC, it is assumed that the sample experiences the same thermal history as designated by the DSC furnace. This may be realized only when the thermal lag between the sample and the furnace is kept minimal. If this assumption is valid, the relation between the crystallization time t and the sample temperature T can be formulated as

$$t = \frac{T_o - T}{\phi} \qquad (3)$$

where ϕ is the cooling rate. According to eq. (3), the horizontal temperature axis observed in a DSC thermogram for the nonisothermal crystallization data can be transformed into the time scale.

Instead of describing the crystallization process with complicated mathematical models, Ziabicki[17–19] proposed a first-order kinetic equation as a means to describe the kinetics of polymeric phase transformation:

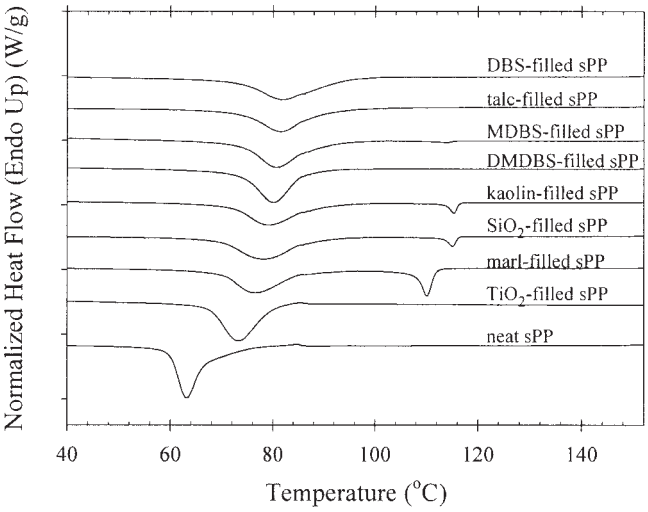

Figure 2 Nonisothermal melt-crystallization exotherms of neat sPP and all of the sPP compounds for a fixed cooling rate of 10°C/min.

TABLE I
Characteristic Data for Nonisothermal Melt-Crystallization Exotherms of Neat sPP and sPP Compounds

ϕ (°C min^{-1})	Neat sPP			DBS-filled sPP			MDBS-filled sPP			DMDBS-filled sPP			Kaolin-filled sPP			Talc-filled sPP			Marl-filled sPP			TiO_2-filled sPP			SiO_2-filled sPP		
	$T_{0.01}$ (°C)	T_p (°C)	$T_{0.99}$ (°C)	$T_{0.01}$ (°C)	T_p (°C)	$T_{0.99}$ (°C)	$T_{0.01}$ (°C)	T_p (°C)	$T_{0.99}$ (°C)	$T_{0.01}$ (°C)	T_p (°C)	$T_{0.99}$ (°C)	$T_{0.01}$ (°C)	T_p (°C)	$T_{0.99}$ (°C)	$T_{0.01}$ (°C)	T_p (°C)	$T_{0.99}$ (°C)	$T_{0.01}$ (°C)	T_p (°C)	$T_{0.99}$ (°C)	$T_{0.01}$ (°C)	T_p (°C)	$T_{0.99}$ (°C)	$T_{0.01}$ (°C)	T_p (°C)	$T_{0.99}$ (°C)
2.5	84.0	77.6	72.7	101.3	92.9	87.1	96.6	90.7	85.8	95.9	90.9	86.2	96.8	90.2	85.5	101.7	93.6	86.7	93.6	88.5	84.9	91.7	86.9	81.8	97.7	90.2	85.9
5	82.6	71.9	66.1	99.9	90.5	82.6	98.5	89.0	81.7	93.0	86.4	80.1	95.4	86.1	78.5	97.7	87.8	78.5	91.1	82.9	77.2	86.8	80.9	75.3	94.9	86.2	79.9
7.5	79.8	67.5	61.1	95.7	85.2	74.8	94.3	83.6	73.5	90.5	82.2	74.7	92.1	81.8	74.6	94.7	84.5	75.2	88.8	80.4	73.6	83.0	76.6	70.3	93.3	82.8	74.3
10	76.0	64.1	58.4	94.0	82.7	72.2	91.2	80.9	68.6	88.1	80.0	72.4	90.5	79.9	71.4	91.8	81.7	72.7	84.3	76.9	69.7	81.9	73.6	66.5	88.1	80.0	72.4
15	72.1	60.0	53.6	89.9	78.1	68.1	89.5	77.9	66.6	83.7	75.9	67.7	82.7	73.7	64.3	88.8	77.2	66.3	82.5	72.5	63.8	78.1	69.3	61.8	82.6	72.1	63.4
20	68.8	57.9	49.7	88.7	76.4	63.2	85.8	73.7	62.6	81.6	72.5	63.2	80.0	69.0	58.8	85.5	74.0	61.1	78.4	67.2	58.2	74.5	65.0	56.3	81.5	69.9	59.7

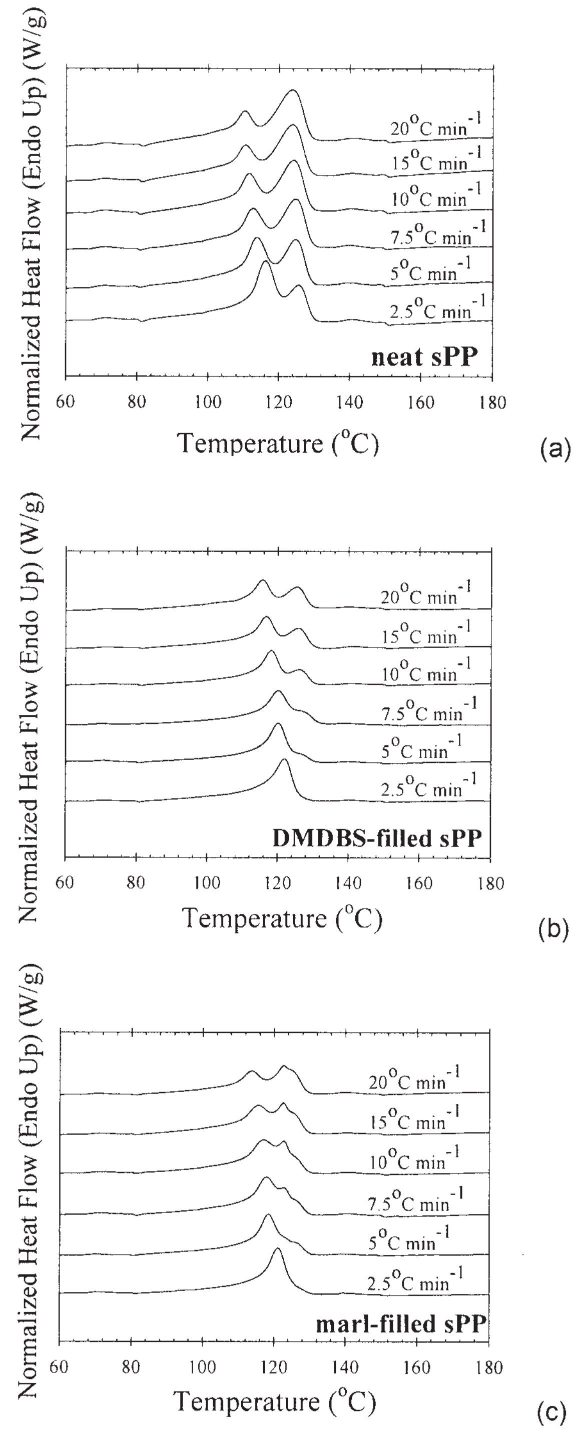

Figure 3 Subsequent melting endotherms of (a) neat sPP and sPP compounded with (b) 1 wt % DMDBS and (c) 5 wt % marl after nonisothermal melt-crystallization for six different cooling rates ranging from 2.5 to 20°C/min.

$$\frac{d\theta(t)}{dt} = K(T)[1-\theta(t)] \quad (4)$$

where $\theta(t)$ is the relative crystallinity as a function of time and $K(T)$ is a temperature-dependent crystallization rate function. In the case of nonisothermal crys-

tallization, $K(T)$ and $\theta(t)$ functions vary and are dependent on the cooling rate used.

For a given cooling condition, Ziabicki[17–19] showed that the crystallization rate function $K(T)$ can be described by a Gaussian function of the following form:

$$K(T) = K_{max}\exp\left[-4\ln 2\,\frac{(T_e - T_{max})^2}{D^2}\right] \quad (5)$$

where T_{max} is the temperature at which the crystallization rate is maximum, K_{max} is the crystallization rate at T_{max}, and D is the width at half-height of the crystallization rate–temperature function. With use of the isokinetic approximation, integration of eq. (5) over the whole crystallizable range of temperatures ($T_g < T < T_m^0$), for a given cooling condition, leads to an important characteristic value for the crystallization ability G of a semicrystalline polymer, which is defined as

$$G = \int_{T_g}^{T_m^0} K(T)dT \approx 1.064 K_{max} D \quad (6)$$

According to an approximate theory,[17] the kinetic crystallizability G characterizes the degree of crystallinity obtained when the polymer is cooled at unit cooling rate from the melting temperature to the glass transition temperature.[19]

In the case of nonisothermal crystallization studies using DSC where cooling rate is a variable, eq. (6) can be applied when the crystallization rate function $K(T)$ is replaced with a derivative function of the relative crystallinity $\dot{\theta}_\phi(T)$ for a particular cooling rate. Therefore, eq. (6) is replaced by

$$G_\phi = \int_{T_g}^{T_m^0} \dot{\theta}_\phi(T)dT \approx 1.064 \dot{\theta}_{max,\phi} D_\phi, \quad (7)$$

where $\dot{\theta}_{max,\phi}$ and $D\phi$ are the maximum crystallization rate and the width at half-height of the derivative relative crystallinity as a function of temperature $\dot{\theta}_\phi(T)$. According to eq. (7), G_ϕ is the kinetic crystallizability at an arbitrary cooling rate ϕ. The kinetic crystallizability at unit cooling rate G can therefore be obtained by normalizing G_ϕ with ϕ (i.e., $G = G_\phi/\phi$). It should be noted that this procedure was first realized by Jeziorny.[20]

EXPERIMENTAL

Materials

Syndiotactic polypropylene used in this work was produced and supplied by AtoFina Petrochemicals (USA) based on a metallocene technology. Some physical properties of the resin, reported by the manufacturer, are density = 0.88 g/cm^3 (ASTM D1505), melt flow index = 2 g/10 min (ASTM D1238), tensile strength = 15 MPa (ASTM D638), tensile modulus = 480 MPa (ASTM D638), elongation at break = 11% (ASTM D790), flexural modulus = 340 MPa (ASTM D638), and notched Izod impact strength = 640 J/m (ASTM D256A).

Inorganic fillers used in this work are kaolin [$Al_2Si_2O_5(OH)_4$; Engelhard Corp. (USA)], talcum [$Mg_3Si_4O_{10}(OH)_2$, Pacific Commo Trading (Thailand)], marl [$CaSiO_3$; Pacific Commo Trading (Thailand)], titanium dioxide [TiO_2; Pacific Commo Trading (Thailand)], and SiO_2 [PPG Siam Silica (Thailand)]. Organic fillers are some sorbitol derivatives such as 1,3 : 2,4-dibenzylidene sorbitol [DBS; Ciba Specialty Chemicals (Switzerland)], 1,3 : 2,4-di-*p*-methyldibenzilidene sorbitol [MDBS; Ciba Specialty Chemicals (Switzerland)], and 1,3 : 2,4-di-*m*,*p*-methylbenzylidene sorbitol [DMDBS; Milliken Asia (Singapore)]. The average particle size of these fillers, measured by a Malvern Instruments Masterizer X particle size analyzer, was found to be the following (in descending order): marl = 42.5 ± 2.0 μm, SiO_2 = 36.4 ± 0.7 μm, DBS = 26.8 ± 1.0 μm, kaolin = 15.1 ± 1.5 μm, talc = 13.9 ± 1.8 μm, DMDBS = 6.7 ± 0.6 μm, TiO_2 = 5.3 ± 1.0 μm, and MDBS = 5.3 ± 0.6 μm.

Sample preparation

All of the fillers used were first dried in a hot-air oven at 60°C for 14 h and then cooled down to room temperature. Each filler was then dry-mixed with sPP pellets in a tumble mixer for 10 min and later compounded in a Collin ZK25 self-wiping, corotating

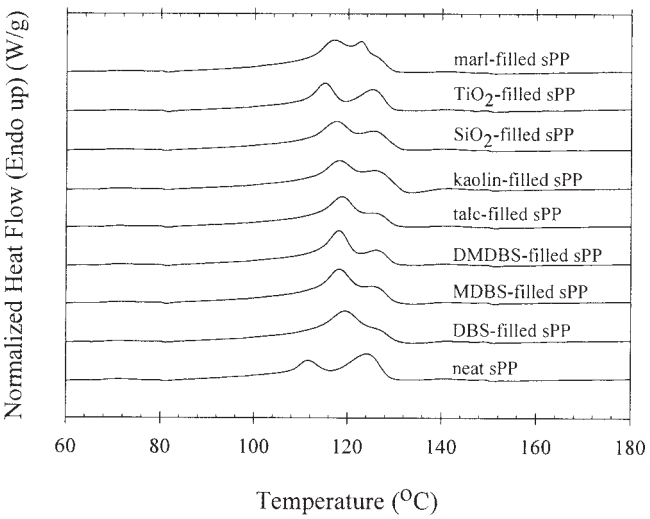

Figure 4 Subsequent melting endotherms (recorded at a fixed heating rate of 20°C/min) of neat sPP and all of the sPP compounds after nonisothermal melt-crystallization for a fixed cooling rate of 10°C/min.

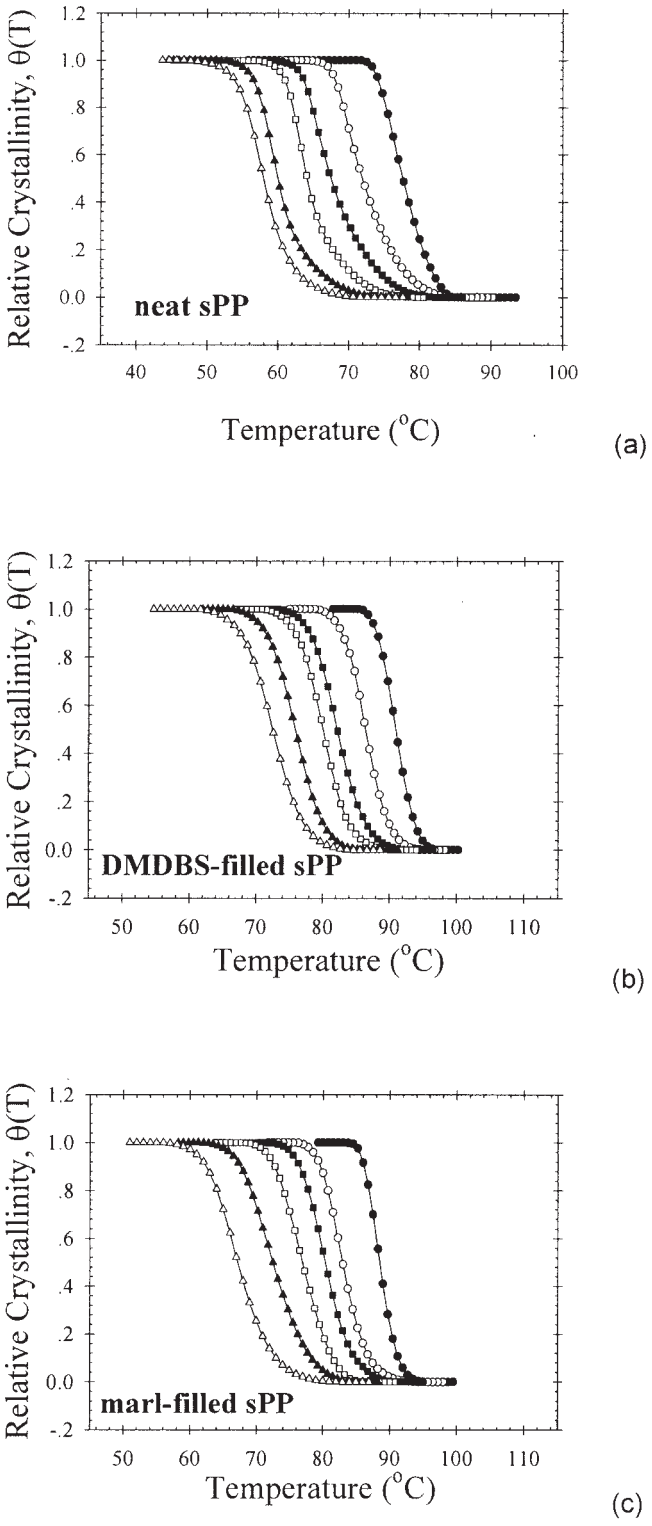

Figure 5 Relative crystallinity as a function of temperature of (a) neat sPP and sPP compounded with (b) 1 wt % of DMDBS and (c) 5 wt % marl for six different cooling rates: (●) 2.5, (○) 5, (■) 7.5, (□) 10, (▲) 15, and (△) 20°C/min.

twin-screw extruder, operating at a screw speed of 50 rpm and the die temperature of 190°C. Due to the limitation on the amount of sPP resin and fillers in possession, only 5% by weight (wt %) of each inorganic filler or 1 wt % of each organic filler was added to the sPP resin. A Planetrol 075D2 pelletizer was used to palletize the extrudate after coming out of the twin-screw kneader.

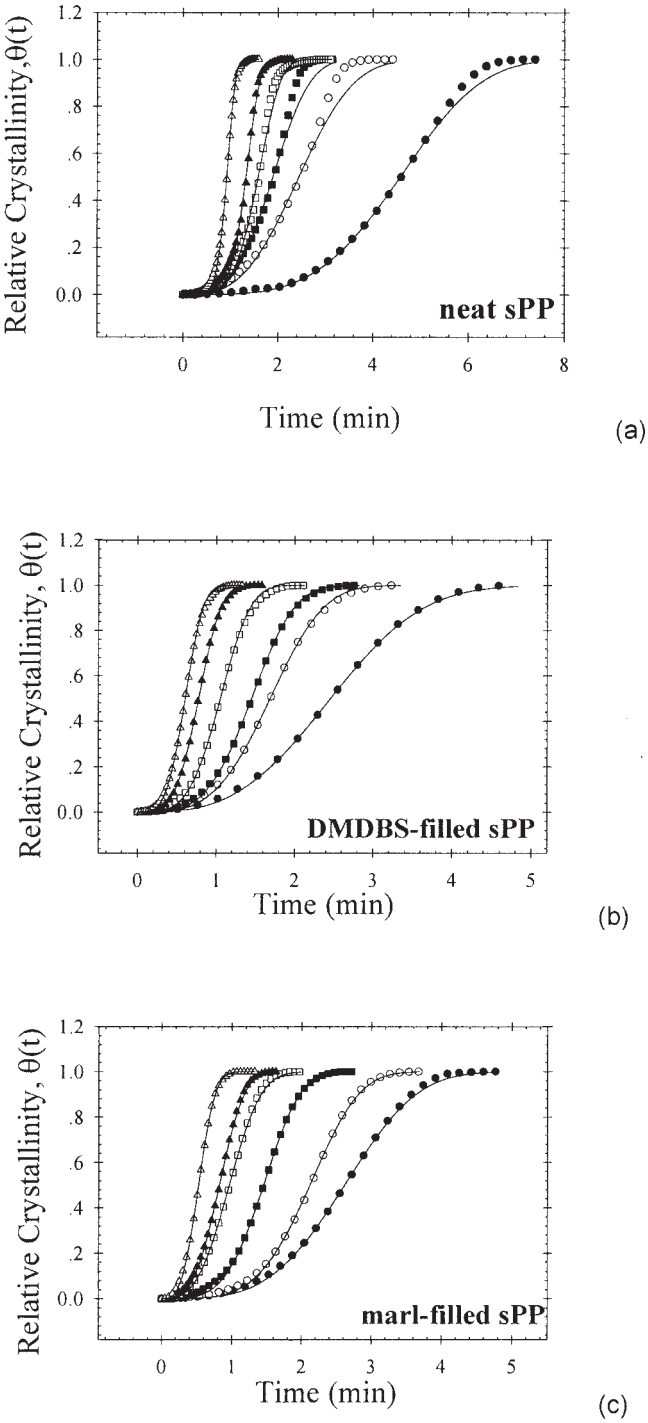

Figure 6 Relative crystallinity as a function of time of (a) neat sPP and sPP compounded with (b) 1 wt % DMDBS and (c) 5 wt % marl for six different cooling rates: (●) 2.5, (○) 5, (■) 7.5, (□) 10, (△) 15, and (▲) 20°C/min. The raw data are shown as various geometrical points, while the Avrami predictions are shown as solid lines.

TABLE II
Nonisothermal Melt-Crystallization Kinetic Parameters for Neat sPP and sPP Compounds Based on Avrami Analysis

	Neat sPP					DBS-filled sPP					MDBS-filled sPP					DMDBS-filled sPP					Kaolin-filled sPP	
ϕ (°C min^{-1})	n_a	K_a (min^{-1})	r^2	$t_{0.5}$ (min)	$t_{0.5}^{-1}$ (min^{-1})	n_a	K_a (min^{-1})	r^2	$t_{0.5}$ (min)	$t_{0.5}^{-1}$ (min^{-1})	n_a	K_a (min^{-1})	r^2	$t_{0.5}$ (min)	$t_{0.5}^{-1}$ (min^{-1})	n_a	K_a (min^{-1})	r^2	$t_{0.5}$ (min)	$t_{0.5}^{-1}$ (min^{-1})	n_a	K_a (min^{-1})
2.5	3.86	0.20	0.9989	4.59	0.22	3.36	0.22	0.9989	4.07	0.25	4.09	0.24	0.9998	3.79	0.26	3.06	0.36	0.9999	2.46	0.41	3.52	0.27
5	3.08	0.36	0.9944	2.47	0.41	3.04	0.38	0.9992	2.33	0.43	3.83	0.37	0.9994	2.49	0.40	3.57	0.54	0.9998	1.69	0.59	3.29	0.41
7.5	3.51	0.48	0.9943	1.91	0.52	3.36	0.49	0.9999	1.82	0.55	3.78	0.49	0.9998	1.88	0.53	3.81	0.63	0.9999	1.45	0.69	3.62	0.53
10	4.68	0.59	0.9964	1.99	0.50	3.20	0.63	0.9997	1.43	0.70	3.87	0.65	0.9994	1.42	0.70	3.92	0.87	0.9997	1.05	0.95	3.55	0.69
15	6.17	0.71	0.9981	1.34	0.75	3.83	0.87	0.9997	1.05	0.96	3.89	0.92	0.9997	0.99	1.01	3.89	1.17	0.9998	0.77	1.30	3.65	1.11
20	6.79	1.03	0.9995	0.77	1.30	3.02	1.22	0.9998	0.73	1.37	4.12	1.12	0.9998	0.81	1.23	3.79	1.50	0.9997	0.60	1.66	4.01	1.26

A film of each compound was prepared by melt-pressing sliced pellets between a pair of transparency films, which were sandwiched between a pair of stainless steel platens in a Wabash V50H compression press. The temperature of the platens was set at 190°C. The molding was preheated for 5 min, before being compressed under an applied clamping force of 10 tons for another 5 min. Later, the film was cooled down, while still in the compression machine, until the temperature of the platens read 40°C. Each film specimen was subjected to thermal analysis.

Differential scanning calorimetry measurements

Nonisothermal melt-crystallization and subsequent melting behavior of sPP samples filled with either an inorganic or an organic filler was investigated using a Perkin–Elmer Series 7 DSC. Temperature calibration was carried out using a pure indium standard (T_m^0 = 156.6°C and ΔH_f = 28.5 J/g) on every other run to ensure accuracy and reliability of the obtained data. To minimize thermal lag between the polymer sample and the furnace, each sample holder was loaded with a disc-shaped specimen, cut from the as-prepared film and weighing around 6.0 ± 0.5 mg. Each sample was used only once and all experimental runs were carried out under nitrogen atmosphere.

The experimental procedure started with heating each sample from 25°C at a rate of 80°C/min to 190°C to set a similar thermal history to each sample. To ensure complete melting, the sample was kept at 190°C for a holding period of 5 min, after which each sample was cooled at a desired rate ϕ, ranging from 2.5 to 20°C/min, to 30°C. The sample was then subjected to heating to observe the subsequent melting behavior (recorded using a heating rate of 20°C/min). Both nonisothermal melt-crystallization exotherms and subsequent melting endotherms were recorded for further analysis.

RESULTS AND DISCUSSION

Nonisothermal melt-crystallization behavior

Figure 1 shows nonisothermal melt-crystallization exotherms of neat sPP and sPP compounded with 1 wt % of DMDBS and 5 wt % of marl for six different cooling rates ranging from 2.5 to 20°C/min. To save some publishing space, the crystallization exothermic traces for other sample types are not shown. For most sample types, a single crystallization exotherm was visible. Only sPP samples compounded with kaolin, marl, and SiO_2 showed double crystallization exotherms. Since the temperature range at which the high-temperature exotherm was observed was too high to be assigned as the crystallization of the primary crystals formed during a cooling scan, only the low-temperature exotherm is considered in this work. According to Figure 1, it is apparent that the exothermic trace for each type of sample became wider and shifted toward lower temperatures with increasing cooling rate used. Other sample types also exhibited a similar trend to that observed in Figure 1.

Figure 2 illustrates nonisothermal melt-crystallization exotherms, recorded at a cooling rate of 10°C/

TABLE III
Nonisothermal Melt-Crystallization Kinetic Parameters for Neat sPP and sPP Compounds Based on Ziabicki's Crystallizability Analysis

	Neat sPP				DBS-filled sPP				MDBS-filled sPP				DMDBS-filled sPP				Kaolin-filled sPP			
ϕ (°C min−1)	$T_{max,\phi}$ (°C)	$\dot{\theta}_{max,\phi}$ (min−1)	D_ϕ	G	$T_{max,\phi}$ (°C)	$\dot{\theta}_{max,\phi}$ (min−1)	D_ϕ	G	$T_{max,\phi}$ (°C)	$\dot{\theta}_{max,\phi}$ (min−1)	D_ϕ	G	$T_{max,\phi}$ (°C)	$\dot{\theta}_{max,\phi}$ (min−1)	D_ϕ	G	$T_{max,\phi}$ (°C)	$\dot{\theta}_{max,\phi}$ (min−1)	D_ϕ	G
2.5	76.2	0.324	7.89	1.09	92.2	0.309	7.45	0.98	90.5	0.384	6.08	0.99	91.0	0.438	5.45	1.02	89.7	0.382	6.18	1.00
5	70.0	0.609	7.53	0.98	89.5	0.472	10.35	1.04	88.2	0.594	7.14	0.90	86.2	0.758	5.87	0.95	85.7	0.573	8.14	0.99
7.5	65.5	0.917	6.58	0.86	86.0	0.666	10.54	0.99	83.0	0.730	9.10	0.94	82.0	0.947	7.17	0.96	81.0	0.773	9.22	1.01
10	63.2	1.606	4.48	0.77	82.0	0.833	11.34	1.01	80.7	0.993	8.28	0.88	80.0	1.309	6.80	0.95	79.2	0.979	9.17	0.96
15	59.2	2.221	5.18	0.82	78.0	1.310	10.13	0.94	77.7	1.395	9.37	0.93	76.0	1.816	7.46	0.96	73.5	1.560	8.78	0.97
20	57.7	2.699	6.16	0.88	76.3	1.461	12.59	0.98	73.3	1.801	9.81	0.94	72.7	2.196	8.10	0.95	68.3	1.952	9.15	0.95
Average				0.90				0.99				0.93				0.96				0.98

TABLE II
Continued

Kaolin-filled sPP			Talc-filled sPP					Marl-filled sPP					TiO_2-filled sPP					SiO_2-filled sPP				
r^2	$t_{0.5}$ (min)	$t_{0.5}^{-1}$ (min^{-1})	n_a	K_a (min^{-1})	r^2	$t_{0.5}$ (min)	$t_{0.5}^{-1}$ (min^{-1})	n_a	K_a (min^{-1})	r^2	$t_{0.5}$ (min)	$t_{0.5}^{-1}$ (min^{-1})	n_a	K_a (min^{-1})	r^2	$t_{0.5}$ (min)	$t_{0.5}^{-1}$ (min^{-1})	n_a	K_a (min^{-1})	r^2	$t_{0.5}$ (min)	$t_{0.5}^{-1}$ (min^{-1})
0.9994	3.35	0.30	2.88	0.23	0.9993	3.89	0.26	3.65	0.35	0.9997	2.81	0.36	3.42	0.36	0.9999	2.47	0.40	3.98	0.23	0.9988	3.92	0.26
0.9993	2.30	0.44	3.38	0.37	0.9996	2.43	0.41	4.25	0.43	0.9997	2.24	0.45	3.71	0.58	0.9999	1.56	0.64	3.66	0.41	0.9995	2.22	0.45
0.9993	1.73	0.58	3.45	0.53	0.9998	1.71	0.59	3.95	0.63	0.9998	1.46	0.68	3.77	0.74	0.9999	1.07	0.93	3.25	0.53	0.9991	1.70	0.59
0.9995	1.32	0.76	3.59	0.72	0.9997	1.26	0.80	3.11	0.92	0.9998	0.97	1.03	3.92	0.83	0.9999	1.10	0.91	3.51	0.64	0.9999	1.40	0.71
0.9999	7.75	0.13	4.08	0.92	0.9996	0.99	1.01	3.35	1.09	0.9997	0.83	1.21	3.95	1.13	0.9999	0.81	1.24	3.22	1.01	0.9994	0.89	1.13
0.9998	0.73	1.37	4.22	1.14	0.9992	0.80	1.25	3.26	1.69	0.9999	0.53	1.89	4.13	1.36	0.9999	0.67	1.49	2.87	1.30	0.9989	0.68	1.47

min, for all of the sample types investigated. Obviously, incorporation of these fillers, though in a very small amount (i.e., 5 wt % for inorganic fillers and 1 wt % for organic fillers), was able to shift the crystallization exotherm toward a higher temperature from that of neat sPP. Among the exotherms shown (note that only the low-temperature exotherm for kaolin-filled, marl-filled, and SiO_2-filled sPP samples was considered), the nonisothermal crystallization exotherm of the DBS-filled sPP sample was found to be in the highest temperature range, followed by that of talc-filled, MDBS-filled, DMDBS-filled, kaolin-filled, SiO_2-filled, marl-filled, TiO_2-filled, and neat sPP samples, respectively. According to the results shown in Figure 2, it can be concluded based on the fillers used and the conditions studied in this work that DBS was the best, while TiO_2 was the worst, nucleating agent for sPP.

To quantify the nonisothermal melt-crystallization data obtained, some characteristic parameters are defined, viz. $T_{0.01}$ = the temperature at 1% relative crystallinity, T_p = the temperature at the maximum crystallization rate or the peak temperature, and $T_{0.99}$ = the temperature at 99% relative crystallinity. $T_{0.01}$ and $T_{0.99}$ are used here to represent the beginning and the ending of the nonisothermal crystallization process. Table I summarizes $T_{0.01}$, T_p, and $T_{0.99}$ values for all of the sample types studied. For a given sample type, all of the $T_{0.01}$, T_p, and $T_{0.99}$ values were found to shift to lower values with increasing cooling rate. The results imply that, the higher the cooling rate, the later the crystallization process began and ended (based on the corresponding positions on the temperature axis).

To compare the nucleation ability among the fillers studied in a quantitative manner, some characteristic parameters are, again, defined, viz. $\Delta T_{0.01}$ = the difference between the $T_{0.01}$ values of an sPP compound and the neat sPP, and ΔT_p = the difference between the T_p values of an sPP compound and the neat sPP. The average $\Delta T_{0.01}$ and ΔT_p values (calculated for a particular sample type from all of the six cooling rates studied) for all of the sPP compounds investigated are as follows: for DSB-filled sPP, they are 17.7 ± 1.3 and 17.8 ± 1.3°C; for MDBS-filled sPP, they are 15.5 ± 1.8 and 16.1 ± 1.7°C; for DMDBS-filled sPP, they are 11.6 ± 0.9 and 14.8 ± 1.0°C; for kaolin-filled sPP, they are 12.4 ± 1.3 and 13.6 ± 1.6°C; for talc-filled sPP, they are 16.2 ± 1.1 and 16.6 ± 0.8°C; for marl-filled sPP, they are 9.2 ± 0.8 and 11.6 ± 1.4°C; for TiO_2-filled sPP, they are 5.5 ± 1.3 and 8.9 ± 0.9°C; and for SiO_2-filled sPP, they are 12.5 ± 1.2 and 13.7 ± 1.7°C. Based on these values, the nucleation ability among these fillers can be ranked from best to worst as follows: DBS > talcum > MDBS > SiO_2 ~ kaolin ~ DMDBS > marl > TiO_2. In other words, talcum and TiO_2 were the best and the worst nucleating agents among the inorganic nucleating agents investigated, while DBS and DMDBS were the best and the worst pair among the organic nucleating agents investigated.

After nonisothermal melt-crystallization, each sample was immediately submitted to heating at a heating rate of 20°C/min to 180°C to observe the subsequent melting behavior. Figure 3 illustrates subsequent melting endotherms of neat sPP and sPP compounded with 1 wt % of DMDBS and 5 wt % of marl after nonisothermal melt-

TABLE III
Continued

Talc-filled sPP				Marl-filled sPP				TiO_2-filled sPP				SiO_2-filled sPP			
$T_{max,\phi}$ (°C)	$\dot{\theta}_{max,\phi}$ (min^{-1})	D_ϕ	G	$T_{max,\phi}$ (°C)	$\dot{\theta}_{max,\phi}$ (min^{-1})	D_ϕ	G	$T_{max,\phi}$ (°C)	$\dot{\theta}_{max,\phi}$ (min^{-1})	D_ϕ	G	$T_{max,\phi}$ (°C)	$\dot{\theta}_{max,\phi}$ (min^{-1})	D_ϕ	G
93.0	0.268	9.16	1.05	88.2	0.492	4.88	1.02	86.7	0.484	4.55	0.94	89.5	0.384	6.14	1.00
87.2	0.510	8.20	0.89	82.2	0.737	6.26	0.98	80.7	0.852	5.32	0.96	85.7	0.626	7.49	1.00
84.0	0.713	9.51	0.96	80.0	0.953	7.13	0.96	76.5	1.078	6.49	0.99	82.0	0.737	9.64	1.01
81.5	1.032	8.47	0.93	76.5	1.128	8.61	1.03	73.2	1.262	7.24	0.97	78.2	0.869	10.51	0.97
77.2	1.461	8.94	0.93	71.7	1.440	9.72	0.99	68.7	1.721	8.10	0.99	71.0	1.319	10.92	1.02
74.0	1.845	9.32	0.91	66.7	2.031	8.83	0.95	64.7	2.154	8.47	0.97	68.3	1.586	12.07	1.02
			0.94				0.99				0.97				1.00

crystallization for six different cooling rates ranging from 2.5 to 20°C/min. To save some publishing space, the melting endothermic traces for other sample types were not shown. Clearly, almost all of the resulting endotherms exhibited double melting peaks, with size and sharpness being dependent on the cooling rate studied and on the type of filler used. Qualitatively, the low-temperature melting endotherm was generally found to increase in its sizes and sharpness and move toward a higher temperature with a decrease in the cooling rate used. On the contrary, the high-temperature melting endotherm generally became smaller with decreasing cooling rate and, for most of the filled systems investigated (with an exception to TiO_2-filled system), it even disappeared altogether when the cooling rate used was lower than 5°C/min. These observations should be a direct result of the increased stability (i.e., thicker lamellae) of the primary crystallites formed during cooling at slow cooling rates.[21]

From Figures 3 and 4, it is only in the case of marl that triple melting peaks were observed for cooling rates greater than or equal to 5°C/min. Since we observed the subsequent melting behavior using a fixed heating rate 20°C/min, it is very interesting to see whether the triple melting peaks can be observed at other heating rates. In so doing, a separate experiment was carried out in which marl-filled sPP samples were nonisothermally crystallized at a fixed cooling rate of 15°C/min and the subsequent melting behavior was observed using various heating rates ranging from 5 to 30°C/min. It was found that the triple melting peaks were clearly visible in all of the subsequent heating thermograms obtained and any change in the heating rate used did not affect the position of the three peaks. It, however, affected the breadth and height of those peaks. At this point, the origin of the triple melting behavior in marl-filled sPP samples was not known and it should be a subject for further investigation.

The effect of the type of filler on the size and sharpness as well as the position of the melting endotherms is well illustrated in Figure 4. Since it was shown elsewhere for sPP[21] that the low-temperature melting endotherm corresponded to the melting of the primary crystals formed, the position and sharpness of this endotherm should correlate with the stability of the lamellae formed during crystallization, which, in nonisothermal crystallization studies, should relate directly to the position of the crystallization exotherm. Based on the position of the crystallization exotherms, the stability of the primary crystals for all of the sample types investigated should be in the following order: DBS-filled > talcum-filled > MDBS-filled > DMDBS-filled > kaolin-filled > SiO_2-filled > marl-filled > TiO_2-filled > neat sPP samples. It is general knowledge that crystals of greater stability (i.e., thicker lamellae) should melt at a higher temperature. According to the results shown in Figure 4, the stability of the primary crystals for all of the sample types studied should be in the following order: DBS-filled > talcum-filled > MDBS-filled ~ DMDBS-filled ~ kaolin-filled > SiO_2-filled > marl-filled > TiO_2-filled > neat sPP samples, which is in excellent agreement with the observation based on the position of the crystallization exotherms.

Avrami analysis

To obtain the relevant kinetic information for the nonisothermal melt-crystallization behavior of all the samples investigated, the raw data such as those shown in Figure 1 need to be converted into relative crystallinity functions of temperature $\theta(T)$ or of time $\theta(t)$, depending on the macrokinetic model used to analyze the data. The conversion from the raw data into $\theta(T)$ functions can be done according to eq. (2) and the conversion from $\theta(T)$ functions into $\theta(t)$ functions can be carried by transforming the temperature scale into the time scale according to eq. (3). Converted $\theta(T)$ and $\theta(t)$ functions for neat sPP and sPP compounded with 1 wt % of DMDBS and 5 wt % of marl after nonisothermal melt-crystallization for six different cooling rates ranging from 2.5 to 20°C/min are shown in Figures 5 and 6, respectively.

An important kinetic parameter that can be taken directly from a $\theta(t)$ function is the half-time of crystallization $t_{0.5}$, which is defined as the time interval from the onset of crystallization to the time at which the crystallization process is half completed. The $t_{0.5}$ values for all of the sample types and cooling conditions studied are summarized in Table II. Obviously, the $t_{0.5}$ value for each sample type was found to increase with decreasing cooling rate, while its inverse value, i.e., the reciprocal half-time of crystallization ($t_{0.5}^{-1}$) (also summarized in Table II), was found to increase with increasing cooling rate, suggesting slow crystallization rates at low cooling rates.

Analysis of the experimental data can be carried out by directly fitting eq. (1) to the $\theta(t)$ functions, such as those shown in Figure 6. In the fitting, only the relative crystallinity data in the range of 10 to 80% were used. The obtained values of the Avrami kinetic parameters (i.e., n_a and K_a) along with the r^2 parameter, signifying the quality of the fitting, for all of the sample types and cooling conditions studied are summarized in Table II.

For all of the sample types studied, the Avrami exponent n_a was found to vary between ~ 2.9 and 6.8. Specifically, for neat sPP, n_a was found to vary between ~ 3.1 and 6.8, which is in good agreement with the values of ~ 2.4 to 5.3 found in an earlier study.[11] For all of the sPP compounds, n_a was found to vary between ~ 2.9 and 4.3. The Avrami crystallization rate constant K_a for a given sample type was found to increase with increasing cooling rate, which is in a similar manner to that of $t_{0.5}^{-1}$. In fact, for any given sample type and cooling rate studied, the values of

both K_a and $t_{0.5}^{-1}$ are very comparable (see Table II). According to the results shown in Table II, addition of these fillers accelerated crystallization, as reflected by the reduction in both K_a values of sPP compounds in comparison with those of neat sPP.

Ziabicki's kinetic crystallizability analysis

Table III summarizes the values of $T_{max,\phi}$, and D_ϕ for neat sPP and sPP filled with various inorganic and organic fillers. The values of $\dot{\theta}_\phi(T)$ and D_ϕ were used to calculate the Ziabicki's kinetic crystallizability G, the values of which are also summarized in Table III. For a given sample type, the temperature at the maximum crystallization rate $T_{max,\phi}$ was found to decrease with increasing cooling rate in a similar manner to the peak temperature T_p summarized in Table I, while both of the maximum crystallization rate ($\theta_{max,\phi}$) and the width at half-height of the derivative relative crystallinity function of temperature D_ϕ were all found to increase with increasing cooling rate. Based on these values, the resulting cooling rate-dependent kinetic crystallizability G_ϕ (results not shown) was an increasing function of the cooling rate, and, after normalizing with the corresponding cooling rate, the kinetic crystallizability G for a given sample type can be calculated and the G values for all of the sample types and the cooling rates studied are summarized in Table III.

The practical meaning of G is the ability of a semicrystalline polymer to crystallize when it is cooled from the melt to the glassy state at a unit cooling rate, hence the higher the G value is, the more readily the polymer can crystallize. According to Table III, the average G value for neat sPP was found to be 0.90, while the average G values for all of the sPP compounds ranged between 0.93 and 1.00, which were all greater than that of neat sPP, suggesting that the sPP compounds were more likely to crystallize than the neat sPP. However, since the average G values for all the sPP compounds were quite close to one another, it was not possible to use the average G values obtained to rank the nucleation ability among the fillers studied.

CONCLUSION

The kinetics of nonisothermal melt-crystallization of syndiotactic polypropylene compounded with 5 wt % of some inorganic fillers (i.e., kaolin, talcum, marl, TiO_2, and SiO_2) and 1 wt % of some organic fillers, which are some sorbital derivatives (i.e., DBS, MDBS, and DMDBS) was investigated and reported for the first time. The nonisothermal melt-crystallization trace for each sample type became wider and shifted toward lower temperatures with increasing cooling rate used. Comparison among the nonisothermal melt-crystallization traces for all of the sample types investigated at a fixed cooling rate of 10°C/min revealed that DBS was the best, while TiO_2 was the worst, nucleating agent for sPP. Careful analysis of the onset temperature shift (i.e., $\Delta T_{0.01}$) suggested the ability of these fillers to nucleate sPP occurs in the following order: DBS > talcum > MDBS > SiO_2 ~ kaolin ~ DMDBS > marl > TiO_2, with DBS being able to shift the crystallization exotherm by ~ 18°C on average, while TiO_2 was able to shift the crystallization exotherm by only ~ 6°C on average, from that of neat sPP. The Avrami analysis revealed the Avrami exponent for sPP compounds was in the range of 2.9 to 4.3, with the values for neat sPP being in the range of 3.1 to 6.8. Lastly, the Ziabicki's crystallizability of sPP compounds was found to range between 0.93 and 1.00, which was greater than that of neat sPP, suggesting the enhancement in the crystallization ability of sPP with addition of these fillers.

The authors acknowledge partial supports received from the Petroleum and Petrochemical Technology Consortium (through a Thai governmental loan from the Asian Development Bank), Chulalongkorn University (through a grant from the Ratchadapisek Somphot Endowment Fund for the foundation of the Conductive and Electroactive Polymers Research Unit), and the Petroleum and Petrochemical College, Chulalongkorn University.

References

1. Ewen, J. A.; Johns, R. L.; Razavi, A.; Ferrara, J. D. J Am Chem Soc 1988, 110, 6255.
2. Natta, G.; Pasquon, I.; Zambelli, A. J Am Chem Soc 1962, 84, 1488.
3. Rodriguez-Arnold, J.; Bu, Z.; Cheng, S. Z. D. J Macromol Sci-Rev Macromol Chem Phys 1995, C35, 117.
4. Schardi, J.; Sun, L.; Kimura, S.; Sugimoto, R. J Plastic Film Sheeting 1996, 12, 157.
5. Sun, L.; Shamshoum, E.; Dekunder G. SPE-ANTEC Proc 1996 1965.
6. Gownder, M. SPE-ANTEC Proc 1998, 1511.
7. Sura, R. K.; Desai, P.; Abhiraman, A. S. SPE-ANTEC Proc 1999, 1764.
8. Guadagno, L.; Naddeo, C.; D'Aniello, C.; Maio, L.; Vitoria, V.; Acierno, D. Macromol Symp 2002, 180, 23.
9. Loos, J.; Bonnet, M.; Petermann J. Polymer 2000, 41, 351.
10. Supaphol, P.; Spruiell J. E. J Appl Polym Sci 2000, 75, 44.
11. Supaphol, P. J Appl Polym Sci 2000, 78, 338.
12. Supaphol, P.; Spruiell J. E. SPE-ANTEC Proc 1999, 1834.
13. Avrami, M. J Chem Phys 1939, 7, 1103.
14. Avrami, M. J Chem Phys 1940, 8, 212.
15. Avrami, M. J Chem Phys 1941, 9, 177.
16. Wunderlich, B. Macromolecular Physics; Academic Press: New York, 1976; p. 147; vol. 2.
17. Ziabicki, A. Appl Polym Symp 1967, 6, 1.
18. Ziabicki, A. Polymer 1967, 12, 405.
19. Ziabicki, A. Fundamental of Fiber Spinning; John Wiley & Sons: New York, 1976; pp. 112–114.
20. Jeziorny, A. Polymer 1978, 19, 1142.
21. Supaphol, P. J Appl Polym Sci 2001, 82, 1083.